JOURNAL OF GUIDANCE, CONTROL, AND DYNAMICS
Vol. 22, No. 4, July–August 1999

Aeroservoelastic Interaction Between Aircraft Structural and Control Design Schemes

Moshe Idan,* Mordechay Karpel,† and Boris Moulin‡
Technion—Israel Institute of Technology, 32000 Haifa, Israel

The behavior of the structural and control systems of flight vehicles are highly coupled through aeroelastic effects. An interaction module was formulated and software was developed to facilitate efficient transfer of models, data and design requirements between the structural and control design schemes. The aeroelastic plant state-space equations are based on a minimum-state rational function approximation of the unsteady force coefficient matrices. The control system is defined in a way that allows incorporation of most general linear control laws in the aeroservoelastic loop, and yet allows efficient control margin and sensitivity computations by separating between changeable gains to other fixed control elements and parameters. Analytical expressions for system stability margins and their sensitivities with respect to structural and control design parameters, which take advantage of the special controller representation form for incorporation in a multidisciplinary design scheme, are presented. A numerical example demonstrates a design task that involves both control synthesis and structural optimization.

Nomenclature

$[A_{(\cdot)}]$, $[B_{(\cdot)}]$, $[C_{(\cdot)}]$, $[D_{(\cdot)}]$ = state-space matrices

$\left[\begin{array}{c|c} A & B \\ \hline C & D \end{array}\right]$ = $[C][s[I]-[A]]^{-1}[B]+[D]$

$[A_{h1,2,3}]$, $[D]$, $[E]$ = rational aerodynamic approximation matrices

b = reference semichord
$\{e_i\}$ = ith unit vector
$[G_{(\cdot)}]$ = controller gain matrices
GM, PM = single input/single output gain and phase margins
$[I]$ = identity matrix
$[L_i]$, $[L_o]$ = multi-input/multi-output uncertainty matrices
$[M_{hc}]$ = mass coupling matrix between control and structural modes
$[M_{hh}]$, $[B_{hh}]$, $[K_{hh}]$ = generalized mass, damping, and stiffness matrices
n_a = number of aerodynamic states
n_h = number of generalized displacements
n_s = number of sensors
$[Q_h]$ = unsteady aerodynamic force coefficient matrix
q = dynamic pressure
$[R]$ = aerodynamic lag matrix
s = Laplace transform variable
$T_{\mathrm{oc}_{j,i}}$ = open–closed loop transfer function
V = true airspeed
$\{v\}$ = design parameters vector
$\{X\}$, $\{Y\}^T$ = left and right eigenvectors
$\{x\}$, $\{u\}$, $\{y\}$ = state, input, and output vectors
$\{x_a\}$ = vector of the aerodynamic augmented states
$\{\delta\}$ = control-surface deflections
$\{\xi\}$ = vector of n_h generalized displacements
$\underline{\sigma}\{\cdot\}$ = minimum singular value
ω = frequency

Subscripts

ac = actuators
ae = open-loop aeroelastics
ase = closed-loop aeroservoelastics
c = control modes or controller
g = gust modes
gco = gain crossover
h = structural modes
oc = open-closed system for single input/single output stability margin calculations
p = open-loop aeroelastics with actuators
pco = phase crossover
v = gain-open aeroservoelastic system

Received 30 March 1998; revision received 30 December 1998; accepted for publication 31 December 1998.

*Senior Lecturer, Faculty of Aerospace Engineering. Associate Fellow AIAA.
†Professor, Faculty of Aerospace Engineering. Senior Member AIAA.
‡Research Associate, Faculty of Aerospace Engineering.

Introduction

THE increasing interaction between aircraft structural and control systems requires the application of aeroservoelastic (ASE) considerations beginning at the preliminary stages of the design process. The interaction affects static and dynamic stability characteristics, performance issues, structural design loads, and handling qualities. It is important to account for the ASE interaction with efficient modeling and analytical schemes that facilitate both automatic multidisciplinary design and convenient application of engineering judgment and regulatory design criteria. On the other hand, common structural and control design methodologies, models, and analytical tools are too different for being implemented in a single code. Therefore, it is desired to develop an ASE computational tool that mediates between the separate design schemes.

The common approach for formulating the dynamic equations of motion for aeroelastic systems uses normal modes of the structure as generalized coordinates. Control surface deflection modes may be added when the interaction with the control system is considered. Complex gust velocity modes may also be introduced to analyze the response of the structural and control systems to continuous gust. The unsteady aerodynamic force coefficients are defined with respect to these modes.

Unsteady aerodynamic modules in common aeroelastic analysis and optimization schemes such as ASTROS[1] and MSC/NASTRAN[2] assume that the structure oscillates harmonically. Transcendental unsteady aerodynamic matrices are calculated for various reduced frequency values. The flutter and gust-response modules use second-order formulations for stability solutions, frequency response, and frequency-domain control synthesis.

The application of various modern control design techniques, simulation, and optimization procedures require the ASE equations of motion to be transformed into a first-order, time-domain (state-space) form.[3,4] This transformation requires the aerodynamic matrices to be approximated by rational functions (ratio of

polynomials) in the Laplace domain. The order of the resulting state-space model is a function of the number of selected modes, the number of aerodynamic approximation roots, and the approximation formula. The main considerations in constructing the model are its size (which affects the efficiency of subsequent analyses), its accuracy, and the model construction efforts.

The purpose of the work presented in this paper was to design and develop an efficient ASE computational module that can support both structural and control automated design schemes by transferring data between the two disciplines and performing relevant ASE analyses. The main features of the ASE module and its interfaces are described in the next section, followed by a section describing the aeroelastic equations of motion and their presentation in state-space form. Then, the proposed control system architecture is presented, followed by the construction of the aeroservoelastic model and the description of the data transfer capabilities of the new aeroservoelastic optimization scheme. Next, formulations of the single input/single output (SISO) and multi-input/multi-output (MIMO) stability margins, which are dictated by the control design requirements and can be incorporated in the multidisciplinary aeroservoelastic optimization, are presented. The derivations also include analytical sensitivities of these stability margins with respect to the structural and controller design parameters, which can be facilitated in the optimization process.

Features of the ASE Module

A block diagram of the ASE module and its interfaces with the control synthesis and structural optimization schemes is given in Fig. 1. It is assumed that the structural optimization code can generate a modal database with normal modes of a baseline structure, the associated generalized stiffness, and mass matrices and their derivatives with respect to the structural design variables, and the frequency-domain generalized unsteady aerodynamic force coefficient matrices used in standard flutter analysis.[1] It is also assumed that the control synthesis scheme is based on state-space formulation, such as the MATLAB® control toolboxes. The ASE module reads the modal database and first constructs the aeroelastic state-space equations of motion. The other activities of the ASE module depend on the user-defined mission. The options are data generation for control synthesis, ASE analysis, behavior sensitivity analysis, and data export for structural optimization.

The data exported for control synthesis may include full or reduced-order aeroelastic state-space model matrices, their variations with respect to structural uncertainties, and aeroelasticity-related design constraints. This data, and the other information transferred between the design modules, are described after the aeroelastic and control formulations. When ASE analysis is requested, the aeroelastic state-space equations are augmented in the ASE module by a linear control system of a general form. The module then calculates open- and closed-loop flutter parameters, control margins associated with the user-defined control architecture, and continuous gust response in statistical terms. These parameters and their analytical derivatives with respect to design variables can then be used by the structural optimization code as design constraints and sensitivities. In addition to the regular structural design parameters, the design variables may include the control system parameters defined as variable gains in the controller formulation, as discussed later and demonstrated in the numerical example.

Aeroelastic System Equations

The time-domain ASE models for stability and response analysis are constructed from the separate models of the aeroelastic plant, the sensors and actuators, the control system, and the gust spectrum filters,[5] all expressed in state-space form. The control system includes the control surfaces driven by actuators, sensors related to the structural degrees of freedom, and a linear MIMO control law that relates the actuator inputs to the sensor signals. The full ASE model can be used for closed-loop flutter analysis, control margin computations, evaluation of the system dynamic response to external excitation, and for flight mechanics.

Most commonly used rational aerodynamic approximation methods are variations of either Roger's classic approximation,[6] which is based on term-by-term least-square fits with common denominator roots, or the minimum-state (MS) method of Karpel,[7] which is based on a more general approximation function with coupling between terms. Consequently, the MS procedure requires computationally heavier, iterative, nonlinear least-square solutions. Recent developments of the MS method[8] improved its accuracy, flexibility, and computational efficiency. The number of aerodynamic states added by the MS method in realistic aeroelastic design models is typically 6–8 times smaller than those added by Roger's approximation with the same level of model accuracy in subsequent analyses. This makes the MS method very attractive in repetitive aeroelastic optimization studies that are based on modes of a baseline structure, and in cases that involve control synthesis.

The MS approximation of the unsteady aerodynamic force coefficient matrices, expanded to the entire Laplace s domain, is

$$[\tilde{Q}_h(s)] = [A_{h0}] + (b/V)[A_{h1}]s + (b^2/V^2)[A_{h2}]s^2 + [D]([I]s - (V/b)[R])^{-1}[E]s \tag{1}$$

where the $[A_{hi}]$ and $[E]$ matrices are column partitioned as

$$[A_{hi}] = \begin{bmatrix} A_{hh_i} & A_{hc_i} & A_{hg_i} \end{bmatrix} \qquad (i = 0, 1, 2)$$

$$[E] = [E_h \quad E_c \quad E_g]$$

where the subscripts h, c, and g relate to the structural, control, and gust modes, respectively. The real coefficient matrices in Eq. (1) are determined by a nonlinear weighted least-square fit[8] of the transcendental unsteady aerodynamic matrices calculated by common frequency-domain flutter codes.[1,2] As shown next, the rational approximation yields a state-space aeroelastic equation of motion where the structural states are augmented by the aerodynamic states. The number of aerodynamic states n_a is equal to the order of $[R]$, which in the MS method is assumed to be diagonal with distinct negative terms.

For clarity and simplicity, the following formulation is for flutter and control margin issues only, for which new developments are presented. Previous works presented extensions of this formulation to static aeroelasticity,[3] continuous gust response,[5] and

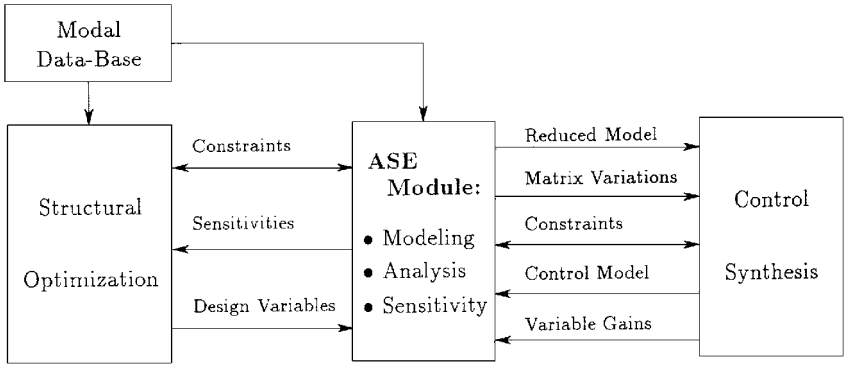

Fig. 1 ASE module feature block diagram.

dynamic response to deterministic excitation.[9] Furthermore, the singular value analysis capabilities of the new ASE module can handle many other MIMO design specifications, such as tracking performance and disturbance rejection.

The state-space open-loop aeroelastic equation of motion resulting from the rational aerodynamic approximation reads

$$\{\dot{\boldsymbol{x}}_{\mathrm{ae}}\} = [A_{\mathrm{ae}}]\{\boldsymbol{x}_{\mathrm{ae}}\} + [B_{\mathrm{ae}}]\{\boldsymbol{u}_{\mathrm{ae}}\} \tag{2}$$

where

$$\{\boldsymbol{x}_{\mathrm{ae}}\} = \begin{Bmatrix} \boldsymbol{\xi} \\ \dot{\boldsymbol{\xi}} \\ \boldsymbol{x}_a \end{Bmatrix}, \qquad \{\boldsymbol{u}_{\mathrm{ae}}\} = \begin{Bmatrix} \delta \\ \dot{\delta} \\ \ddot{\delta} \end{Bmatrix}, \qquad [A_{\mathrm{ae}}] = \begin{bmatrix} 0 & [I] & 0 \\ -[\bar{M}]^{-1}\left[K_{hh} + qA_{hh_0}\right] & -[\bar{M}]^{-1}\left[B_{hh} + (qb/V)A_{hh_1}\right] & -q[\bar{M}]^{-1}[D] \\ 0 & [E_h] & (V/b)[R] \end{bmatrix}$$

$$[B_{\mathrm{ae}}] = \begin{bmatrix} 0 & 0 & 0 \\ -q[\bar{M}]^{-1}\left[A_{hc_0}\right] & -(qb/V)[\bar{M}]^{-1}\left[A_{hc_1}\right] & -[\bar{M}]^{-1}\left[M_{hc} + (qb^2/V^2)A_{hc_2}\right] \\ 0 & [E_c] & 0 \end{bmatrix}, \qquad [\bar{M}] = [M_{hh}] + (qb^2/V^2)\left[A_{hh_2}\right]$$

The number of states in Eq. (2) is $2n_h + n_a$. Open-loop flutter analysis is performed by extracting the eigenvalues of matrix $[A_{\mathrm{ae}}]$ for various values of the dynamic pressure at constant Mach number. Flutter occurs when the real part of one of the eigenvalues becomes positive.

The outputs of the aeroelastic plant are sensor signals. It is assumed here that the sensors measure either structural displacements, velocities, or accelerations, and that the measurements are perfect. Sensor dynamics can be modeled in series with the outputs of the ideal sensors in the control part of the model discussed in the sequel. In general, the output of n_s sensor signals can be expressed by

$$\{\boldsymbol{y}_{\mathrm{ae}}\} = [C_{\mathrm{ae}}]\{\boldsymbol{x}_{\mathrm{ae}}\} + [D_{\mathrm{ae}}]\{\boldsymbol{u}_{\mathrm{ae}}\} \tag{3}$$

The dynamic model of the actuator driving the ith control surface is specified by a transfer function with three poles and no zeros. This pole-zero difference is justified on physical grounds: a second-order difference representing the control surface deflection response to a force input and a first-order lag used to model the realistically limited bandwidth of the actuator. Because of this order difference, δ_i, $\dot{\delta}_i$, and $\ddot{\delta}_i$ can be defined as independent states in the actuator state-space model, and thus used directly as inputs to Eq. (2) and in connections to acceleration sensors. The third-order actuators models are considered here as part of the aeroelastic plant. Higher-order actuator dynamics can be defined by connecting additional transfer functions in series, as part of the control system model discussed in the next section.

The actuators are modeled by

$$\{\dot{\boldsymbol{x}}_{\mathrm{ac}}\} = [A_{\mathrm{ac}}]\{\boldsymbol{x}_{\mathrm{ac}}\} + [B_{\mathrm{ac}}]\{\boldsymbol{u}_{\mathrm{ac}}\} \tag{4a}$$

$$\{\boldsymbol{y}_{\mathrm{ac}}\} = [C_{\mathrm{ac}}]\{\boldsymbol{x}_{\mathrm{ac}}\} \tag{4b}$$

where

$$\{\boldsymbol{y}_{\mathrm{ac}}\} = \begin{Bmatrix} \delta \\ \dot{\delta} \\ \ddot{\delta} \end{Bmatrix}$$

The third-order actuator model can be realized in the phase plane, so that the state vector $\{\boldsymbol{x}_{\mathrm{ac}}\}$ equals to the output vector $\{\boldsymbol{y}_{\mathrm{ac}}\}$, simplifying Eq. (4b) to $[C_{\mathrm{ac}}] = [I]$.

The state-space realizations of the actuators are augmented to the aeroelastic model of Eq. (2). The result is the plant equation

$$\{\dot{\boldsymbol{x}}_p\} = [A_p]\{\boldsymbol{x}_p\} + [B_p]\{\boldsymbol{u}_p\} \tag{5a}$$

where $\{\boldsymbol{u}_p\}$ is the vector of actuator inputs, and

$$\{\boldsymbol{y}_p\} = [C_p]\{\boldsymbol{x}_p\} \tag{5b}$$

where $\{\boldsymbol{y}_p\}$ is the vector of sensor signals. Note the lack of the feedthrough term in Eq. (5b), which results from the strictly proper model of the actuator dynamics previously discussed.

Control Model

The ASE interaction model discussed in this paper is formulated to handle any linear time-invariant control system, and enables changes in its parameters during a multidisciplinary design and optimization. Such parameterization of the controller is obtained by defining its architecture as an interconnection of three types of basic control elements, the parameters of which are fixed, and a variable gain matrix, the parameters of which are subject to various ASE system analyses (e.g., stability margin calculations) and can be altered during the multidisciplinary design and optimization. The three basic elements are SISO transfer functions, MIMO state-space models, and zero-order junctions (JNC) or constant gain elements. Any linear controller with nonfixed parameters can be easily parameterized as an interconnection of these three elements and the variable gain matrix. For example, the bandwidth of a low-pass filter can be modeled as a unity gain feedback loop with an integrator (SISO element) and a variable gain (the bandwidth) in its forward path.

The interconnections within the fixed control elements and between them and the aeroelastic (AE) system can be either fixed or through the variable gain matrix. A generic example of such controller setup is demonstrated schematically in Fig. 2. The elements of the variable gain matrix can be used in stability margin analyses. Moreover, these variable gains only (and not the whole controller) can be grouped with the AE system parameters for multidisciplinary design and optimization. The suggested controller setup, which separates its fixed and variable parts, can potentially reduce the computational load of the optimization process. Unnecessary recalculation of the entire ASE model because of changes in the design parameters (both in the AE model and the controller variable gains) can be avoided by constructing a model of the *fixed* part of the control system only once, and by reusing it in the ASE model reconstruction throughout the optimization process. Clearly, if the control system is updated as a result of significant changes in the AE model, the entire ASE model has to be reconstructed.

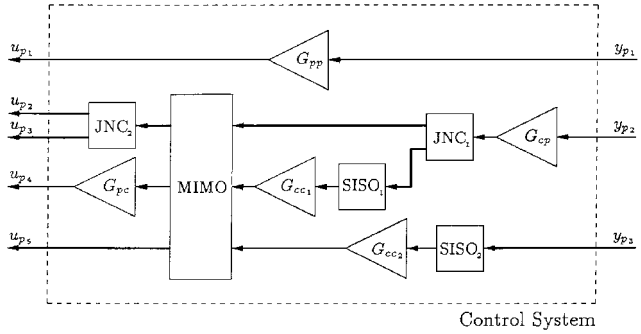

Fig. 2 Control system interconnection model—a typical example. Thick lines represent fixed connections. The y_{p_i} ($i = 1, 2, 3$) are the sensor signals and u_{p_i} ($i = 1, \ldots, 5$) are outputs to the actuators.

The main advantage of the proposed controller setup is its flexible structure suitable to model any general linear control system, while grouping all of the controller variations in a single matrix. This greatly simplifies the subsequent analyses and the overall ASE optimization setup.

To construct the control system model, all of its elements are first combined into one (not yet connected) state-space model. The inner fixed connections of the control system are applied first to produce the fixed part of the controller, which is independent of the controller variable gains and clearly not affected by the aerodynamic and structural design variables. In state-space formulation this fixed controller is given by

$$\{\dot{\boldsymbol{x}}_c\} = [A_c]\{\boldsymbol{x}_c\} + [B_c]\{\boldsymbol{u}_c\} \tag{6a}$$

$$\{\boldsymbol{y}_c\} = [C_c]\{\boldsymbol{x}_c\} + [D_c]\{\boldsymbol{u}_c\} \tag{6b}$$

Aeroservoelastic Model

The ASE model is obtained by connecting the AE model of Eqs. (5) with the control system of Eqs. (6) through fixed and variable gain connections, shown schematically in Fig. 3. The fixed connections are represented by the matrices $[I_{cp}]$ and $[I_{pc}]$, for which a nonzero entry (i, j) of one represents a fixed connection between the jth input and the ith output. The $[I_{cp}]$ represents connections from the AE model (p) sensor outputs to the controller (c) inputs, while $[I_{pc}]$ represents connection of the controller commands to the AE model actuator inputs. Similarly, the matrices $[G_{cp}]$, $[G_{cc}]$, $[G_{pc}]$, and $[G_{pp}]$ include the variable gain connections between the AE plant and the control system. The nonzero elements in these matrices can be used in various stability margin evaluations and can also be included, in addition to the aerodynamic and structural design parameters, as variables of a multidisciplinary optimization procedure. For presentation purposes (not necessarily required in the actual implementation), the plant and controller inputs and outputs are grouped according to their use in fixed and variable gain connections, as depicted in Fig. 3.

First, the *gain-open* ASE model, which is obtained by using only the fixed connections within the interconnection setup (see Fig. 3), is constructed:

$$\{\dot{\boldsymbol{x}}_v\} = [A_v]\{\boldsymbol{x}_v\} + [B_v]\{\boldsymbol{u}_v\} \tag{7a}$$

$$\{\boldsymbol{y}_v\} = [C_v]\{\boldsymbol{x}_v\} + [D_v]\{\boldsymbol{u}_v\} \tag{7b}$$

where

$$[A_v] = \begin{bmatrix} A_p + B_{p_2} I_{pc} D_{c_{22}} I_{cp} C_{p_2} & B_{p_2} I_{pc} C_{c_2} \\ B_{c_2} I_{cp} C_{p_2} & A_c \end{bmatrix}$$

$$[B_v] = \begin{bmatrix} B_{p_1} & B_{p_2} I_{pc} D_{c_{21}} \\ 0 & B_{c_1} \end{bmatrix}, \qquad [C_v] = \begin{bmatrix} C_{p_1} & 0 \\ D_{c_{12}} I_{cp} C_{p_2} & C_{c_1} \end{bmatrix}$$

$$[D_v] = \begin{bmatrix} 0 & 0 \\ 0 & D_{c_{11}} \end{bmatrix}$$

This model is widely used for subsequent SISO- and MIMO-type stability margin evaluations that can be incorporated in the structural optimization process as stability constraints. The sensitivities of the stability margins needed for the optimization are evaluated analytically using the model of Eqs. (7), as will be demonstrated later.

The closed-loop ASE model is obtained by relating the input vector $\{\boldsymbol{u}_v\}$ to the output vector $\{\boldsymbol{y}_v\}$ via the variable gain matrix $[G_v]$:

$$\{\boldsymbol{u}_v\} = [G_v]\{\boldsymbol{y}_v\} \tag{8}$$

where

$$[G_v] = \begin{bmatrix} G_{pp} & G_{pc} \\ G_{cp} & G_{cc} \end{bmatrix}$$

leading to the closed-loop ASE equations of motion

$$\{\dot{\boldsymbol{x}}_{\text{ase}}\} = [A_{\text{ase}}]\{\boldsymbol{x}_{\text{ase}}\} \tag{9}$$

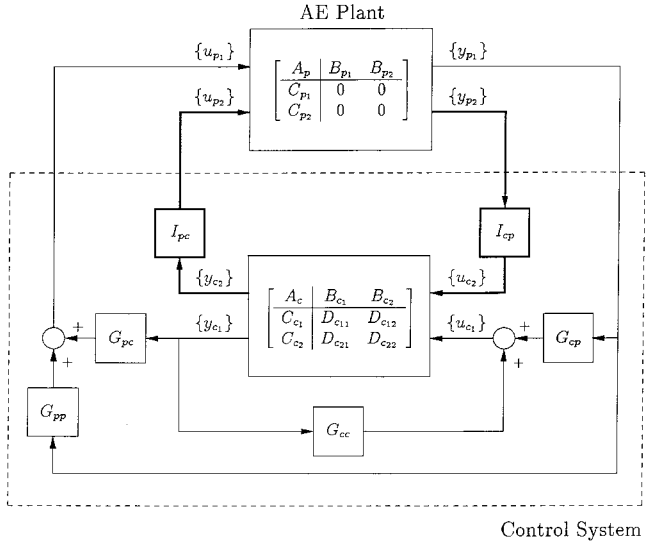

Fig. 3 ASE interconnection model; thick lines represent fixed connections.

with

$$[A_{\text{ase}}] = [A_v] + [B_v][G_v][I - D_v G_v]^{-1}[C_v]$$

The closed-loop state-space realization of the ASE system can be used in the structural optimization scheme for calculating flutter [similar to the open-loop flutter calculations discussed earlier following Eq. (2)] and dynamic response constraints, and their sensitivities to the structural design variables and to the control gains.[3,5] Multidisciplinary design criteria is introduced to the structural optimization scheme by adding the control margin consideration formulated in the following sections.

Both the open- and closed-loop models presented before can be easily extended to include external gust inputs. That would require augmentation of the state vector to incorporate the gust models (e.g., the rational approximation of the von Kármán model dynamics[5]), whereas the input vector would be extended to include the driving signals to those models. An ASE model with gust allows calculation of the system response to wind inputs and forms the basis for synthesis and analysis of a controller with improved closed-loop disturbance attenuation requirements. Such synthesis and analysis, and other stability and airframe performance features, can be addressed more effectively in a separate control design scheme.

Data Transfer Between Design Schemes

The module that interconnects the structural and control design schemes is designed to facilitate efficient highly coupled design cycles with automatic data transfer between the schemes. The data processed by the interaction module and transferred from the structural design scheme to the control one includes:

1) Reduced-size versions of the plant equations for nominal- and extreme-case designs (this is explained later);

2) Sensitivities of these matrices and their allowable variations with respect to structural design variables for robust-control design;

3) Aeroelastic effectiveness of the global aerodynamic coefficients; and

4) Values of all of the control gains changed in the structural process.

The data processed by the interaction module and transferred from the control design scheme to the structural one include:

1) Control system defined in terms of the components of Fig. 2;

2) Definition of control design variables as changeable gains in the structural design process and the associated move limits;

3) Control design constraints to be satisfied in the structural scheme.

The number of structural modes taken into account in the structural optimization scheme is typically considerably larger than that required for an adequate control design. Size reduction techniques such as truncation, static residualization, and dynamic residualization can be applied to the plant model of Eqs. (5) when

the model is exported to the control design scheme. The evaluation of the relative importance of retaining the structural modes can be based on the physical weighting of Ref. 7. The size reduction techniques are presented and demonstrated in Ref. 10.

Aeroservoelastic interaction affects almost all of the structural and control design constraints. However, it is not necessary to include all of them in the two design schemes. Stress alleviation requirements, for example, can be represented in the control design by limiting the wing-root bending moments in gust response or static maneuvers. Maneuvering performance and control authority requirements, on the other hand, can be represented in the structural design by assigning aeroelastic effectiveness constraints. Highly coupled issues such as flutter should be addressed in both schemes.

The derivatives of the plant matrices and their allowable variations may be needed for robust control design. The issue of robust controller design is beyond the scope of this paper. Some robustness requirements, however, can be integrated in the structural scheme in terms of the stability margins discussed next. Moreover, the singular value computation capabilities of the new interaction module provides the framework for specifying additional performance and disturbance rejection design criteria not covered in the current presentation.

Stability Margins

The constraints specified by the controller designer may include SISO and MIMO stability margin requirements to handle model uncertainty, robust performance specifications, and disturbance rejection properties. To enhance the optimization process, sensitivities of these constraints with respect to structural, aerodynamic, and controller parameters are required. When possible, analytical evaluation of the various constraints and sensitivities is advantageous from numerical standpoint. The stability margin analysis, which covers both SISO and MIMO techniques, evaluates closed-loop ASE system stability for variation in the controller variable gain matrix $[G_v]$ of Eq. (8). The sensitivities of these margins with respect to the structural and control variable parameters are derived analytically.

SISO Stability Margins and Sensitivities

The SISO stability analysis addresses the case of uncertainties or possible gain and phase variations in one element of the controller gain matrix $[G_v]$, e.g., $G_{v_{i,j}}$. For the evaluation of the SISO stability margins for $G_{v_{i,j}}$, the loop connecting y_{v_j} to u_{v_i} is opened and the SISO transfer function between the resulting open points is multiplied by the nominal $\bar{G}_{v_{i,j}}$. This operation is performed by first closing a MIMO control loop similar to Eq. (8) with the (i, j) element of $[G_v]$ set to zero, denoted by $[G_v^{(i,j)=0}]$, and then multiplying the result by $\bar{G}_{v_{i,j}}$. The final *open–closed* loop transfer function is given by

$$T_{\mathrm{oc}_{j,i}}(s) = \left[\begin{array}{c|c} A_{\mathrm{oc}} & b_{\mathrm{oc}_i} \\ \hline c_{\mathrm{oc}_j} & d_{\mathrm{oc}_{j,i}} \end{array}\right] \tag{10}$$

where

$$[A_{\mathrm{oc}}] = [A_v] + [\tilde{B}_v][\tilde{C}_v], \qquad \left\{b_{\mathrm{oc}_i}\right\} = [B_v]\{\boldsymbol{e}_i\} + [\tilde{B}_v]\left\{\tilde{D}_{v_i}\right\}$$

$$\left[c_{\mathrm{oc}_j}\right] = \bar{G}_{v_{i,j}}\{\boldsymbol{e}_j\}^T[\tilde{C}_v], \qquad d_{\mathrm{oc}_{j,i}} = \bar{G}_{v_{i,j}}\{\boldsymbol{e}_j\}^T\left\{\tilde{D}_{v_i}\right\}$$

$$[\tilde{B}_v] = [B_v]\left[G_v^{(i,j)=0}\right], \qquad [\tilde{C}_v] = [\bar{D}_v]^{-1}[C_v]$$

$$\left\{\tilde{D}_{v_i}\right\} = [\bar{D}_v]^{-1}[D_v]\{\boldsymbol{e}_i\}, \qquad [\bar{D}_v] = \left[I - [D_v]\left[G_v^{(i,j)=0}\right]\right]$$

and $\{\boldsymbol{e}_i\}$ and $\{\boldsymbol{e}_j\}$ are the ith and the jth unit vectors. The SISO stability margins for $G_{v_{i,j}}$ can be easily computed using standard techniques and software, while using the open–closed loop transfer function of Eq. (10).

Sensitivities of the controller gain $G_{v_{i,j}}$ SISO stability margins are constructed analytically for the structural design parameters and for the controller variable gains, all grouped in the vector $\{\boldsymbol{v}\}$.

The sensitivities of the upper and lower gain margins $GM_{u,l}$ expressed in decibels are given by

$$\frac{\partial GM_{u,l}\,[\mathrm{dB}]}{\partial v_i} = \frac{20/\ell n 10}{GM_{u,l}}\frac{\partial GM_{u,l}}{\partial v_i} \tag{11}$$

where $\partial GM_{u,l}/\partial v_i$ is the regular (not in decibel) gain margin sensitivity, given in the following.

The gain margin sensitivities with respect to $G_{v_{i,j}}$ are given simply by

$$\frac{\partial GM_{u,l}}{\partial G_{v_{i,j}}} = -\frac{GM_{u,l}}{\bar{G}_{v_{i,j}}} \tag{12}$$

or, in decibels, by

$$\frac{\partial GM_{u,l}\,[\mathrm{dB}]}{\partial G_{v_{i,j}}} = -\frac{20/\ell n 10}{\bar{G}_{v_{i,j}}} \tag{13}$$

To compute the gain margin sensitivities with respect to the other design variables v_i, the matrix $[A_{GM_{u,l}}]$ is constructed:

$$\left[A_{GM_{u,l}}\right] = \left[[A_{\mathrm{oc}}] + \frac{GM_{u,l}}{1 - d_{\mathrm{oc}_{j,i}}GM_{u,l}}\left\{b_{\mathrm{oc}_i}\right\}\left[c_{\mathrm{oc}_j}\right]\right] \tag{14}$$

Denoting ω^u_{pco} and ω^l_{pco} as the phase crossover frequencies that correspond to the upper and lower gain margins, respectively, $\jmath\omega^{u,l}_{\mathrm{pco}}$ is an eigenvalue of $[A_{GM_{u,l}}]$. The gain margin sensitivities are obtained by differentiating these imaginary axis eigenvalues, while imposing that the perturbed eigenvalues are purely imaginary. This derivation leads to the gain margin sensitivities given by

$$\frac{\partial GM_{u,l}}{\partial v_i} = -\frac{\mathrm{Re}\left(\{\boldsymbol{Y}\}^T\left(\partial A_{GM_{u,l}}/\partial v_i\right)\{\boldsymbol{X}\}/\{\boldsymbol{Y}\}^T\{\boldsymbol{X}\}\right)}{\mathrm{Re}\left(\{\boldsymbol{Y}\}^T\left(\partial A_{GM_{u,l}}/\partial GM_{u,l}\right)\{\boldsymbol{X}\}/\{\boldsymbol{Y}\}^T\{\boldsymbol{X}\}\right)} \tag{15}$$

where $\{\boldsymbol{X}\}$ and $\{\boldsymbol{Y}\}^T$ are right and left eigenvectors of $[A_{GM_{u,l}}]$ and

$$\frac{\partial A_{GM_{u,l}}}{\partial GM_{u,l}} = \frac{1}{\left(1 - d_{\mathrm{oc}_{j,i}}GM_{u,l}\right)^2}\left\{b_{\mathrm{oc}_i}\right\}\left[c_{\mathrm{oc}_j}\right]$$

The sensitivity $\partial A_{GM_{u,l}}/\partial v_i$ is constructed using Eq. (10), where the sensitivities of $[A_v]$, $[B_v]$, and $[C_v]$ are computed as in Ref. 3, with $\partial[D_v]/\partial v_i = 0$.

To compute the sensitivities of the upper and lower phase margins $PM_{u,l}$ with respect to the design variable vector $\{\boldsymbol{v}\}$, the matrix $[A_{PM_{u,l}}]$ is constructed:

$$\left[A_{PM_{u,l}}\right] = \left[[A_{\mathrm{oc}}] + \frac{1}{\exp(\jmath PM_{u,l}\,[\mathrm{rad}]) - d_{\mathrm{oc}_{j,i}}}\left\{b_{\mathrm{oc}_i}\right\}\left[c_{\mathrm{oc}_j}\right]\right] \tag{16}$$

where $PM_{u,l}\,[\mathrm{rad}]$ is the phase margin expressed in radians. Note that $[A_{PM_{u,l}}]$ is complex and that $\jmath\omega^{u,l}_{\mathrm{gco}}$ is its eigenvalue, where ω^u_{gco} and ω^l_{gco} are the gain crossover frequencies, which correspond to the upper and lower phase margins, respectively. The analytical derivation of the phase margin sensitivities is similar to the gain margin sensitivities derivation, leading to

$$\frac{\partial PM_{u,l}}{\partial v_i} = -\frac{\mathrm{Re}\left(\{\boldsymbol{Y}\}^T\left(\partial A_{PM_{u,l}}/\partial v_i\right)\{\boldsymbol{X}\}/\{\boldsymbol{Y}\}^T\{\boldsymbol{X}\}\right)}{\mathrm{Re}\left(\{\boldsymbol{Y}\}^T\left(\partial A_{PM_{u,l}}/\partial PM_{u,l}\,[\mathrm{rad}]\right)\{\boldsymbol{X}\}/\{\boldsymbol{Y}\}^T\{\boldsymbol{X}\}\right)}\cdot\frac{180}{\pi} \tag{17}$$

where $\{\boldsymbol{X}\}$ and $\{\boldsymbol{Y}\}^T$ are right and left eigenvectors of $[A_{PM_{u,l}}]$ and

$$\frac{\partial A_{PM_{u,l}}}{\partial PM_{u,l}\,[\mathrm{rad}]} = -\frac{\jmath\exp(\jmath PM_{u,l}\,[\mathrm{rad}])}{\left(\exp(\jmath PM_{u,l}\,[\mathrm{rad}]) - d_{oc_{j,i}}\right)^2}\left\{b_{\mathrm{oc}_i}\right\}\left[c_{\mathrm{oc}_j}\right]$$

Again, the sensitivity $\partial A_{PM_{u,l}}/\partial v_i$ is constructed using Eq. (10) and results of Ref. 3.

MIMO Stability Margins and Sensitivities

There is no unique definition for MIMO stability margins, and any particular choice is dictated by the designer's personal preference. In

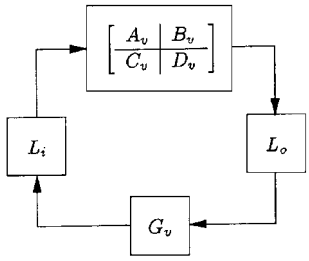

Fig. 4 MIMO stability margin evaluation setup.

the sequel we have chosen one of such definitions, which most naturally extend the intuitive SISO stability margins. However, it should be pointed out that any formulation can be incorporated in the ASE interaction model using similar techniques. Thus, following Ref. 11, the MIMO stability margins are defined by introducing ASE system uncertainties at the plant input or output as described in Fig. 4.

The input and output MIMO stability margins are defined with respect to uncertainties (variations) in the matrices $[L_i]$ and $[L_o]$, which are assumed to be diagonal, i.e.,

$$[L_i] = \text{diag}\left[g_l^i e^{j\phi_l^i}\right], \qquad l = 1, 2, \ldots, N_i \tag{18a}$$

$$[L_o] = \text{diag}\left[g_k^o e^{j\phi_k^o}\right], \qquad k = 1, 2, \ldots, N_o \tag{18b}$$

where N_i and N_o are the number of inputs and outputs, respectively, to the ASE model. At the nominal condition, $g_l^i = g_k^o = 1$ and $\phi_l^i = \phi_k^o = 0 \ \forall\, l, k$, i.e., $[L_i] = I_{N_i \times N_i}$ and $[L_o] = I_{N_o \times N_o}$. Sufficient conditions for a guaranteed gain margin $\bar{g}^i$ and phase margin $\bar{\phi}^i$ at any input to the gain-open ASE plant are[11]

$$[(1 - 1/\bar{g}^i)^2 + 2(1 - \cos\bar{\phi}^i)/\bar{g}^i]^{\frac{1}{2}} < \underline{\sigma}\{I - G_v P_v\} \tag{19a}$$

or

$$[(1 - \bar{g}^i)^2 + 2\bar{g}^i(1 - \cos\bar{\phi}^i)]^{\frac{1}{2}} < \underline{\sigma}\left\{I - [G_v P_v]^{-1}\right\} \tag{19b}$$

where

$$[P_v(s)] = [C_v][sI - A_v]^{-1}[B_v] + [D_v]$$

and $\underline{\sigma}\{\cdot\}$ is the minimum singular value of the argument matrix evaluated at $s = j\omega \,\forall\, \omega \geq 0$. Sufficient conditions for output gain and phase margins are similar to the inequalities of Eqs. (19) except for replacing the $[G_v P_v]$ terms with $[P_v G_v]$.

The inequalities of Eqs. (19) on the ASE system minimum singular values can serve as MIMO stability margins in the multidisciplinary optimization process. Their sensitivities with respect to a design parameter v_i are computed analytically from the singular value derivative expression

$$\frac{\partial\underline{\sigma}\{H\}}{\partial v_i} = \text{Re}\left(\{\boldsymbol{U}\}^* \frac{\partial H}{\partial v_i}\{\boldsymbol{V}\}\right) \tag{20}$$

where $\{\boldsymbol{U}\}$ and $\{\boldsymbol{V}\}$ are, respectively, the left and right normalized singular vectors of the matrix $[H]$, corresponding to the minimum singular value $\underline{\sigma}\{H\}$, while $\{\cdot\}^*$ denotes a complex conjugate transpose. In the ASE MIMO case,

$$[H] = [I] - [G_v]\left[[C_v][sI - A_v]^{-1}[B_v] + [D_v]\right] \tag{21}$$

and the evaluation of the derivative $\partial\underline{\sigma}\{H\}/\partial v_i$ facilitates the sensitivities of $[A_v]$, $[B_v]$, $[C_v]$, and $[D_v]$ that were discussed earlier in the SISO margin section.

Numerical Example

The numerical example is based on a generic Advanced Fighter Aluminum (AFA) ASTROS model with an all movable horizontal tail and four control surfaces on each wing, where only the two trailing-edge control surfaces are used for maneuvering. A top view of the unsteady aerodynamic doublet-lattice model is shown in Fig. 5. The structural model consists of 1276 grid points and 4449 elements, and has 3762 free degrees of freedom with symmetric boundary conditions and 3797 with antisymmetric ones. The top view of the entire aircraft structural finite-element model is shown in Fig. 6. A top view of the wing box divided into 13 design zones is shown in Fig. 7. The thickness of the upper and lower skins in each design zone are used as design variables, leading to a total of 26 structural design variables. More details on this model can be found in Ref. 12, where the model is optimized for minimum weight, with stress and static aeroelastic constraints.

A simplified design scenario is presented to demonstrate the new ASE module in a multidisciplinary design process, which involves structural and control system optimization. The design started with a basic structural model with uniform thickness of 0.5 in. assigned to all the design skin element, with a total weight of 779.5 lb. Preliminary structural and control designs were then performed independently based on this model. The control system was then combined in the ASE module with the aeroelastic model and a final tuning of the structural and control design variables was performed using

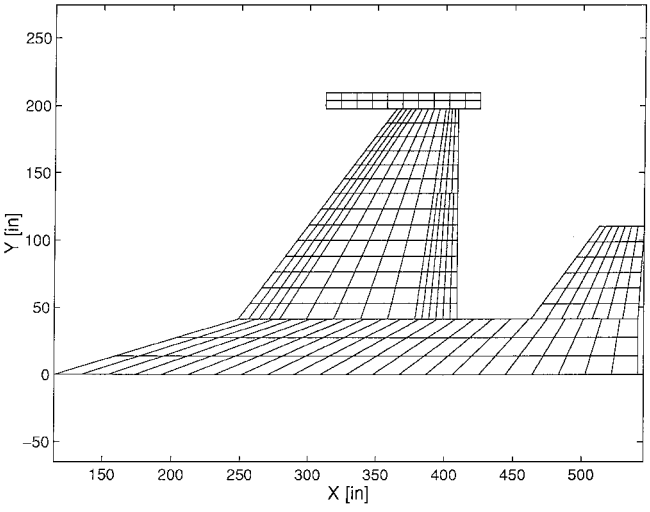

Fig. 5 AFA unsteady aerodynamic model.

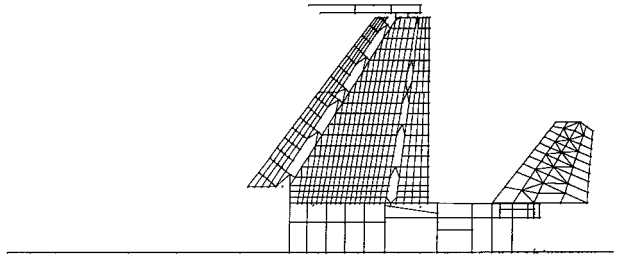

Fig. 6 AFA structural model.

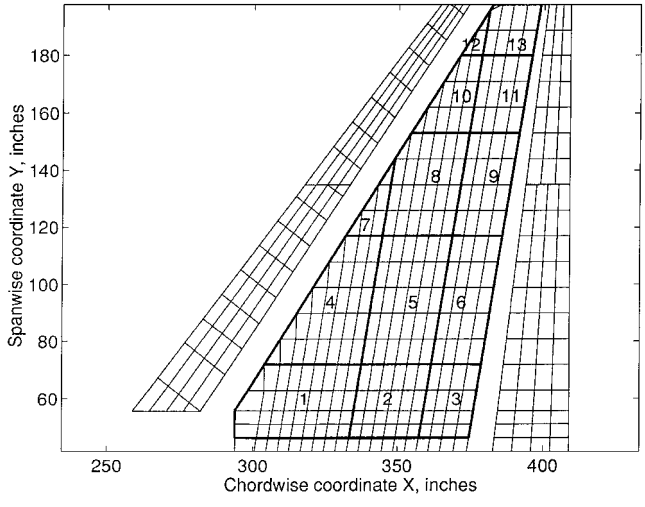

Fig. 7 AFA wing structural model.

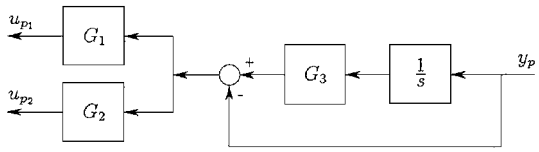

Fig. 8 Control system interconnection model for the numerical example.

ASTROS with stress, flutter, and control system constraints considered simultaneously.

The preliminary structural design was aimed at minimizing the weight of the wing-box skin, with stress constraints generated by a single case of a symmetric 9 *g* pull-up maneuver at Mach 0.95. The only control surface used for maneuver trim in this study was the all-movable horizontal stabilizer. The von Misses stresses of the skin elements were constrained to less than 36,700 psi. The total weight of the wing-box skin was reduced to 474.7 lb with skin thicknesses varying between 0.67 in. at the wing root to 0.09 in. at the wing tip.

The ASTROS generated modal database of the basic (uniform thickness) structural model with antisymmetric boundary conditions was used by the ASE module to construct reduced-order plant state-space equations (5) for a sea level and Mach 0.9 flight. This model, used for preliminary controller design, included 10 structural states, representing 5 low-frequency modes including one of rigid-body roll, 4 aerodynamic states, and 6 actuator states, representing the two trailing-edge actuators. The plant inputs were the commands u_{p_1} and u_{p_2} to the outboard and inboard trailing edge actuators, respectively. The only output y_p was a roll-rate reading near the fuselage center.

The controller design was aimed at achieving low-frequency toll rate performance subject to control deflections limits and stability requirements. In this study, a simple control architecture, which, as shown in Fig. 8, included a low-pass filter and two gains, was used. As an initial attempt, the controller gains were set equal, i.e., $G_1 = G_2$. This attempt failed because it caused a severe instability (flutter) that involved the rolling mode and the first wing-bending mode. The solution was to assign opposite signs to G_1 and G_2, such that the inboard aileron rolls the aircraft while the outboard control surface (which is not very effective in roll because of aeroelastic effects) suppresses flutter. The parameter G_3 defines the low-pass filter bandwidth introduced to avoid high-frequency flutter/spillover.

The preliminary control synthesis defined a baseline system with $G_1 = 0.06$, $G_2 = -0.3$, and $G_3 = 10$. These gains are to be used as design variables in a combined structure-control optimization. The control synthesis process also defined optimization constraints: 1) gain limits of $0 \le G_1 \le 0.1$ and $-0.5 \le G_2 \le 0$ that specify the limited control authority; 2) $G_3 \ge 5$; 3) SISO stability margins of $GM > 6$ dB and $PM > 45$ deg; and 4) the low-frequency roll performance constraint expressed as $G_{p_1} G_1 + G_{p_2} G_2 < -4$, where G_{p_1} and G_{p_2} are the dc gains of the plant from the actuators u_{p_1} and u_{p_2} to the sensor output y_p, which are affected of course by the structural parameters. The control model and the design constraints were transferred to the ASE module for optimization.

The combined optimization run was based on ASTROS, integrated with the new ASE module. The baseline optimization model was the stress-designed structure augmented by the preliminary control model. This time, the state vector included 60 structural states, 10 aerodynamic states, 6 actuator states, and 1 control state. Closed-loop control margin analysis at the design flight point, and flutter analysis at velocities up to 1.2 times that of the design point, showed that the flutter and control margin requirements are not satisfied, which calls for a integrated structural-control optimization run.

To allow a clear view of the ASE effects on the structural design, the combined optimization was performed with the ASE design constraints only, while the stress requirements are assumed to be satisfied by assigning the stress-designed gains as minimal structural gauges. The 26 structural and 3 control design variables were allowed to change simultaneously in a standard ASTROS optimization process, augmented by the new controller gain variables, the ASE constraints, and their sensitivities. All of the constraints were satisfied by increasing the structural weight by 9.2 lb and changing the gains to $G_1 = 0.0054$, $G_2 = -0.4686$, and $G_3 = 5$. Virtually all the added weight resulted from increasing the thickness of the upper and lower skins of Zone 6 (see Fig. 7), in which the inboard actuator is located. This increased the aeroelastic effectiveness of the inboard aileron and increased the flutter speed associated with its dynamic characteristics. From the control system standpoint, the low-pass filter bandwidth was decreased to suppress high frequency spillover further, enabling an increase in the main actuator gain G_2. In addition, lower gain G_1 could now be used because of improved flutter characteristics.

Conclusions

The aeroservoelastic interactive design concept presented in this study facilitates an efficient multidisciplinary design optimization with highly coupled structural and control systems through aeroelastic effects. Being based on common state-space formulation, the structural and control schemes can exchange models, data, and design criteria automatically and efficiently. The modular control modeling allows an easy inclusion of any linear control system in the structural design and the treatment of selected control parameters as design variables. In the other direction, the export of reduced-size plant models facilitates control design that considers basic aeroelastic characteristics. The incorporation of multivariable stability margins along with the more traditional SISO stability margins allows convenient implementation of the proposed methodology in existing industrial design procedures. Even though the paper discussed and demonstrated flutter, stability margin, and basic performance analyses only, the synthesis and analysis tools incorporated in the new aeroservoelastic interactive design concept can be readily applied for additional design criteria such as gust response, performance and disturbance rejection requirements, and controller robustness to plant uncertainties.

Acknowledgments

This work was supported in part by the U. S. Air Force Research Laboratories/Air Vehicles (AFRL/VA) under a Small Business Technology Transfer Phase II contract through Zona Technology and the University of Oklahoma. The technical advice received from V. B. Venkaya of AFRL/VA is gratefully acknowledged.

References

[1] Neill, D. J., Johnson, E. H., and Confield, R., "ASTROS—A Multidisciplinary Automated Structural Design Tool," *Journal of Aircraft*, Vol. 27, No. 12, 1990, pp. 1021–1027.

[2] Climent, H., and Johnson, E. H., "Aeroelastic Optimization Using MSC/NASTRAN," *Proceedings of the International Forum on Aeroelasticity and Structural Dynamics*, Association Aéronautique et Astronautique de France, Paris, 1993, pp. 1097–1116.

[3] Karpel, M., "Multidisciplinary Optimization of Aeroservoelastic Systems Using Reduced-Size Models," *Journal of Aircraft*, Vol. 29, No. 5, 1992, pp. 939–946.

[4] Livne, E., Schmit, L. A., and Friedmann, P. P., "Integrated Structure/Control/Aerodynamic Synthesis of Actively Controlled Composite Wings," *Journal of Aircraft*, Vol. 30, No. 3, 1993, pp. 387–394.

[5] Zole, A., and Karpel, M., "Continuous Gust Response and Sensitivity Derivatives Using State-Space Models," *Journal of Aircraft*, Vol. 31, No. 5, 1994, pp. 1212–1214.

[6] Roger, K. L., "Airplane Math Modeling and Active Aeroelastic Control Design," CP-228, AGARD, 1977, pp. 4.1–4.11.

[7] Karpel, M., "Time-Domain Aeroservoelastic Modeling Using Weighted Unsteady Aerodynamic Forces," *Journal of Guidance, Control, and Dynamics*, Vol. 13, No. 1, 1990, pp. 30–37.

[8] Karpel, M., and Strul, E., "Minimum-State Unsteady Aerodynamic Approximations with Flexible Constraints," *Journal of Aircraft*, Vol. 33, No. 6, 1996, pp. 1190–1196.

[9] Karpel, M., and Presente, E., "Structural Dynamic Loads in Response to Impulsive Excitation," *Journal of Aircraft*, Vol. 32, No. 4, 1995, pp. 853–861.

[10] Karpel, M., "Reduced-Order Aeroelastic Models via Dynamic Residualization," *Journal of Aircraft*, Vol. 27, No. 5, 1990, pp. 449–455.

[11] Mukhopadhyay, V., "Control Law Synthesis and Stability Robustness Improvement Using Constrained Optimization Techniques," *Control and Dynamic Systems*, Vol. 32, Academic, New York, 1990, pp. 163–205.

[12] Karpel, M., Moulin, B., and Love, M. H., "Modal-Based Structural Optimization with Static Aeroelastic and Stress Constraints," *Journal of Aircraft*, Vol. 34, No. 3, 1997, pp. 433–440.